Available online at www.sciencedirect.com

SciVerse ScienceDirect

Ceramics International 39 (2013) 6475–6480

CERAMICS INTERNATIONAL

www.elsevier.com/locate/ceramint

Fabrication and characterization of Mn-doped CuO thin films by the SILAR method

Y. Gülen[a], F. Bayansal[b,*], B. Şahin[b], H.A. Çetinkara[b], H.S. Güder[b]

[a]Department of Physics, Faculty of Arts and Sciences, Marmara University, Istanbul, Turkey
[b]Department of Physics, Faculty of Arts and Sciences, Mustafa Kemal University, Hatay, Turkey

Received 6 December 2012; received in revised form 24 January 2013; accepted 24 January 2013
Available online 5 February 2013

Abstract

Thin films of un-doped and Mn-doped CuO nanostructures have been deposited on glass substrates via the SILAR method. The morphological, compositional, structural and optical properties of the films have been investigated by scanning electron microscopy, energy dispersive spectroscopy, X-ray diffraction analysis and UV–vis spectrophotometry. The analyzed results indicate that the obtained films consist of plate-like nanostructures. From the EDS analysis it is seen that Mn-doping concentration affects the shapes of the nanostructures. XRD results show that all of the films have monoclinic structure. From the room temperature UV–vis analysis it is found that the optical band gap of the films increases with increasing Mn-doping concentrations.

Keywords: Copper oxide (CuO); Mn doping; Band gap; Transmittance; SILAR

1. Introduction

Transition metal oxides in the nanoscale region are of great interest in the current research because of their interesting properties with a variety of applications. Among them, cupric oxide (CuO) is an important p-type transition metal oxide with a narrow band gap (E_g=1.2–1.9 eV) [1–3]. CuO has received considerable attention in recent years due to its unique properties and wide application range in gas sensors [4], biosensors [5], solar cells [6], high T_c superconductors [7], lithium ion batteries [8], catalysts [9], etc. Many efforts have been made to fabricate nanostructured CuO materials, including nanoparticles [10], nanorods [11], nanowires [12], nanoplates [13], and nanotubes [14], to enhance its performance. It is known that shape controlled morphologies highly affect the properties of the nanomaterials. Besides this, a number of elements can be used as doping elements to enhance the physical and chemical properties of materials. Although a number of researches have been done on doping of nanostructured films, it ~~is~~ still remains a challenge to achieve high quality of crystalline films with excellent physical and chemical properties of doped CuO nanostructures.

Among transition metal oxides, copper oxide has drawn a lot of attention because of its excellent performance as a catalyst. Mn is known as an excellent catalyst too. Many researches on the mixed oxide catalysts containing manganese oxides or copper oxides were carried out [15]. From the literature survey it was found that there are a few reports on Mn-doped bulk and/or nanostructured CuO [12,16,17]. Gao et al. have synthesized Mn-doped CuO nanowires by oxidizing Mn–Cu alloys for 20 h and have investigated the magnetic properties of the nanowires [12]. Yang et al. have synthesized Mn-doped CuO powder and pellet samples by the coprecipitation method followed by annealing at 1000 °C for 10 h and have investigated the magnetic properties of the samples too [16]. Zhang et al. have deposited Mn-doped CuO thin films by radio frequency magnetron sputtering. The ceramic targets of $Mn_xCu_{1-x}O$ used were synthesized by using the standard solid-state reaction technique [17]. They have investigated the AC susceptibility, electrical transport and magnetotransport properties of the films. But to our best

*Corresponding author. Tel.: +90 326 2455845; fax: +90 326 2455867.
E-mail addresses: fbayy@hotmail.com, fbayansal@gmail.com (F. Bayansal).

0272-8842/$ - see front matter © 2013 Elsevier Ltd and Techna Group S.r.l. All rights reserved.
http://dx.doi.org/10.1016/j.ceramint.2013.01.077

knowledge there is no report on the morphological, structural and optical properties of Mn-doped nanostructured CuO films.

Many deposition techniques like spin-coating [18], thermal evaporation [19], microwave irradiation [20], electrodeposition [21], solution growth [22], etc. were employed for coating of CuO films. Furthermore, Mn-doped CuO has been synthesized by oxidizing Mn–Cu alloys, coprecipitation and RF magnetron sputtering techniques [12,16,17]. The methods used in these reports take much time and need high annealing temperatures which make them expensive. On the other hand successive ionic layer adsorption and reaction (SILAR), a solution-based technique, is a promising technique because it is a simple, safe, environmental friendly and low cost technique. The method is also capable of producing metal oxide films at relatively low temperatures.

In the present paper, we present a simple approach to synthesize CuO nanostructures onto amorphous substrates (microscope glass slides) with different doping concentrations of Mn by the SILAR method for the first time. The morphological, compositional, structural and optical properties of the films have been investigated and correlated with each other by scanning electron microscopy (SEM), energy dispersive spectroscopy (EDS), X-ray diffraction (XRD) analysis and UV–vis spectrophotometry.

2. Experimental details

Un-doped and Mn-doped CuO nanostructures were deposited on glass substrates by the SILAR method. The experiments were carried out in a solution containing Cu^{2+} (for un-doped samples) or Cu^{2+}:Mn^{2+} (for doped samples) ions. The raw materials used in the experiments were analytical grade reagents, purchased from Sigma-Aldrich Company and Merck KGaA and used without further purification. Un-doped samples were synthesized as follows: first, 0.1 M copper chloride solution was prepared with copper(II) chloride dehydrate ($CuCl_2 \cdot 2H_2O$) and 100 ml double distilled water (18.2 MΩ cm). Then the solution was stirred in a magnetic stirrer at room temperature for a few minutes in order to get a transparent and well-dissolved solution. After stirring, pH value of the solution was adjusted to ~10.0 by adding aqueous ammonia and then the solution was heated up to 90 °C. During the experiments the temperature was kept constant. In order to get 1–2 μm thick films, 10 cycles of SILAR were applied. An SILAR cycle can be described as follows: the substrates were dipped into the solution and kept there for 30 s. Then they were taken out from the bath and immediately dipped into hot water (90 °C) for another 30 s. Finally the films were dried at room temperature for a day. After drying, the samples were cleaned in an ultrasonic bath for 5 min in order to loose bigger and tightly bonded particles. For the doped samples the same procedure was applied but this time, different concentrations (1, 3 and 5 at%) $Mn(NO_3)_2$ was added to 0.1 M copper chloride solutions. The rest of the experiments were maintained as the same.

A Phlips XL30S FEG scanning electron microscope (SEM) was operated at an acceleration voltage of 15 kV for morphological images. The compositions of Mn ions have been investigated through energy dispersive spectroscopy (EDS). The crystal structures of the samples were examined by a

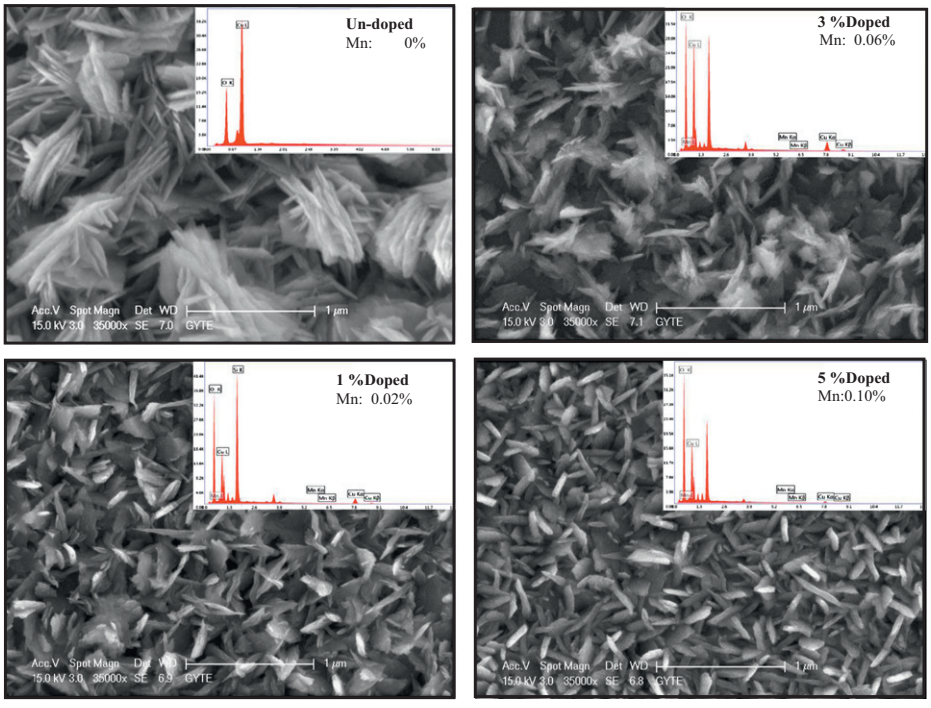

Fig. 1. SEM images and EDS results of un-doped and Mn-doped CuO films.

Rigaku SmartLab X-ray diffractometer (XRD: Cu Kα radiation, $\lambda = 1.540056$ Å). A scan rate of 0.01°/s was applied to record the patterns in the 2θ range of 30–80°. Optical studies were conducted at room temperature by using a Thermo Scientific Genesys 10 S UV–vis spectrophotometer. The optical spectral range was 190–1100 nm.

3. Results and discussion

3.1. Morphological studies

The surface morphology of un-doped and Mn-doped CuO films was characterized by scanning electron microscopy. Mn concentrations in the films were investigated by energy dispersive spectroscopy. Fig. 1 shows the surface morphology and elemental distribution (insets) of the un-doped and Mn-doped films. From these graphs it was seen that the Mn concentrations of 1%, 3% and 5% in the growth solutions provided doping values of 0.02, 0.06 and 0.10 at% Mn in the films respectively. Because of this linear behavior between the doping concentration of the growth solutions and the doping percentages of the films one can conclude that higher concentrations of Mn ions in the growth solution will result in higher doping levels of Mn in the CuO films. As seen from the SEM figures the obtained films are crack free with nano-sized particles. The surface morphology of the films almost remained unchanged while the Mn concentration increased. All of the films consist of plate-like nanostructures as previously reported [13,22]. The increase in the Mn concentration in the films increases the thickness but decreases the length of the plates. Thicknesses of the nanostructures, listed in Table 1, are found to be 24, 32, 34 and 47 nm and lengths of the nanostructures are found to be 700, 270, 250 and 200 nm for un-doped, 1%, 3% and 5% Mn doped films respectively. As we will see in the following sections this change will affect deeply the band gap of the films. From the XRD analysis it was seen that the intensities of the preferential planes were decreased by a big amount with Mn doping. Also there are no extra peaks due to Mn metal, other oxides or any copper manganese phase, indicating that the samples are in single phase. Thus the Mn ion was understood to have substituted the Cu sites. It is also known that the crystal growth rate is bigger in the preferential directions than the other directions. Substitutions of Mn ions to the Cu sites may cause a decrease in the growth of the preferential planes.

3.2. Structural studies

The crystal structure and the orientation of the films have been investigated by using a Rigaku SmartLab X-ray diffractometer (XRD: Cu Kα radiation, $\lambda = 1.540056$ Å) and the results are depicted in Fig. 2. The XRD patterns of un-doped and Mn-doped (1%, 3% and 5%) films were obtained at an operating voltage and current of 40 keV and 30 mA, respectively. The 2θ range of 30–80° was recorded at the scan rate of 0.01°/s. From the figure it was understood that all of the films are polycrystalline in nature, exhibiting monoclinic structures. The peak positions were indexed to (110), ($\bar{1}$11), (111), ($\bar{2}$02), (020), ($\bar{1}$13), ($\bar{3}$11) and (220) planes and the peak positions were found to be in accordance with the JCPDS [card: 01-080-0076] of CuO. But from the XRD data it is evident that there are no additional peaks due to Mn or oxides of Mn which means that the substitution of Cu atoms by Mn atoms has not changed the monoclinic structure of CuO or the peaks belonging to Mn atoms were very weak that they disappeared in the noise signal. It is found that the intensities of ($\bar{1}$11) and (111) peaks are much stronger than those of other peaks which indicate that they are preferential crystal planes of the nanostructures. Mn doping (even in small percentages) caused a large decrease in the ($\bar{1}$11) and (111) peak intensities at first. But then, as the doping concentration was increased the ($\bar{1}$11) and (111) peak intensities also increased slowly. These diffraction patterns show that the intensities of diffraction peaks declined as Mn was doped, i.e. Mn doping within CuO films caused the crystallinity to degenerate. On the other hand increasing Mn doping has a generative effect on the crystallinity. It is evident from the XRD data that there are no extra peaks due to manganese metal, other oxides or any copper manganese phase, indicating that the as-synthesized samples are in single phase. The Mn ion was understood to have substituted the Cu site without changing the monoclinic structure.

The average grain size (D) of Mn doped CuO films was calculated from the peak full width at the half maximum

Table 1
Thickness and length of the plates, band gap and grain size of the films as a function of Mn concentration.

Mn concentration of the growth solutions (at%)	Mn concentration of the films (at%)	Thickness of the plates (nm)	Length of the plates (nm)	E_g (eV)	Average grain size (nm)
–	–	24	700 ± 110	1.42	9.94
1	0.02	32	270 ± 20	1.98	7.83
3	0.06	34	250 ± 28	2.08	8.21
5	0.10	47	200 ± 22	2.20	9.76

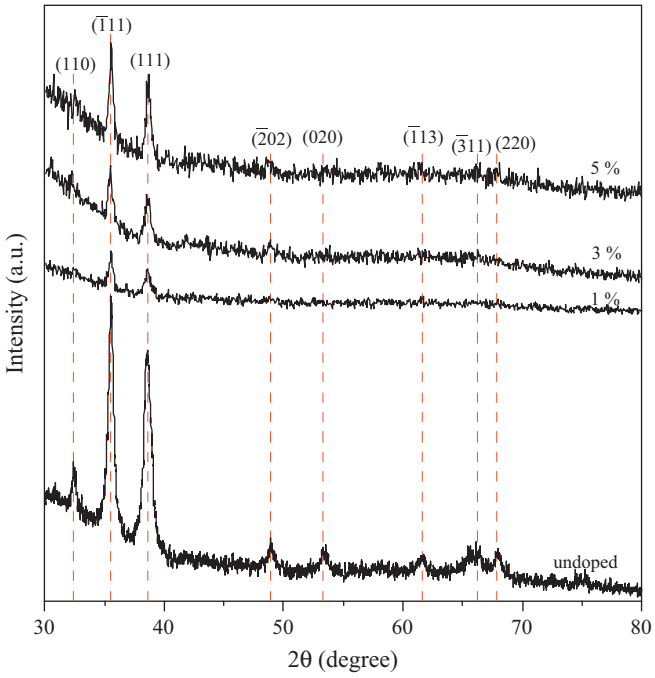

Fig. 2. X-ray diffraction patterns of un-doped and Mn-doped CuO films.

(FWHM) of a peak (β), using the Scherrer formula [23]

$$D = \frac{k\lambda}{\beta\cos\theta} \quad (1)$$

where k is the shape factor ($\sim$0.9), λ is the wavelength of X-ray radiation, θ is Bragg's angle of the peaks and β is the angular width of peaks at FWHM. Calculated average grain sizes (D) of the CuO films are given in Table 1. An introduction of 0.02 at% in Mn concentration resulted in a decrease in grain size from 9.94 nm to 7.83 nm. Further increase in Mn concentration resulted in increases of grain sizes (8.21 nm for 0.06 at% of Mn and 9.76 nm for 0.10 at% of Mn).

3.3. Optical studies

The optical properties of pure and Mn-doped CuO films were studied to investigate the effect of doping on the optical transmittance and band gap energies. The room temperature transmission spectra of un-doped and Mn-doped films in the wavelength range of 400–1100 nm are shown in Fig. 3. Un-doped CuO does not transmit the wavelengths under 700 nm and it transmits the higher wavelengths at small percentages (maximum of 10%). But as seen from the figure, Mn incorporation to the films increases the transmittance and it reaches the value of $\sim$80% at 0.10 at% Mn doping. The samples do not have sharp absorption edges which yield in between 500 and 800 nm. In order to calculate the band gap energies the absorption characteristics of the films were recorded in the wavelength range of 190–1100 nm. CuO is known to be a direct-allowed semiconductor. For the direct allowed transitions it is well known that the theory of optical absorption gives the relation between absorption coefficient (α) and photon energy ($h\upsilon$) as [24]

$$(\alpha h\upsilon)^2 = B(h\upsilon - E_g) \quad (2)$$

where B is an energy independent constant and E_g is the optical band gap. Fig. 4 shows the graph of $(\alpha h\upsilon)^2$ versus photon energy ($h\upsilon$) as a function of Mn-doping percentages. By using this graph the direct gap values can be determined by extrapolating the straight line portion. The E_g value of

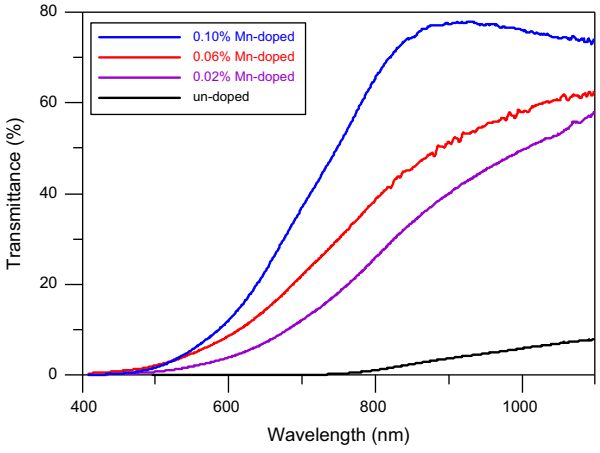

Fig. 3. Optical transmittance spectra of un-doped and Mn-doped CuO films.

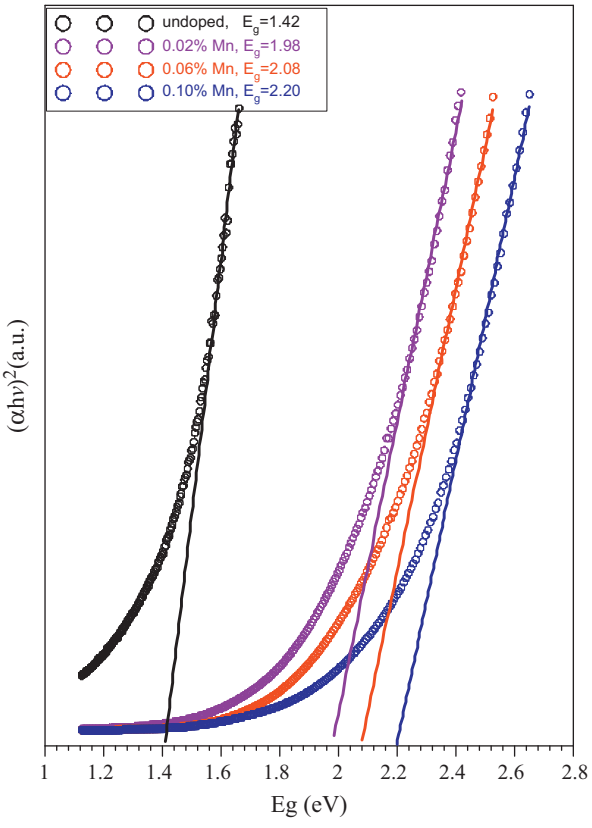

Fig. 4. Comparison of $(\alpha h\upsilon)^2$ versus $h\upsilon$ plots of un-doped and Mn-doped CuO films.

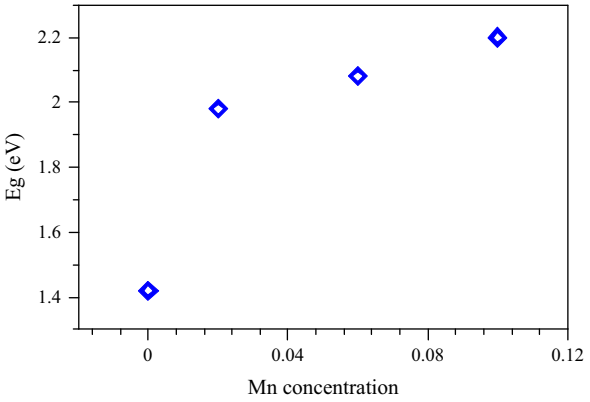

Fig. 5. Band gap values of the CuO films as a function of Mn concentration.

un-doped CuO film was found to be 1.42 which is in a good agreement with [22]. The intercept values on the energy axis were found to be 1.98, 2.08 and 2.20 for 0.02, 0.06 and 0.10 at% Mn-doped CuO films respectively. It was found that the optical band gap was gradually increased with Mn-doping. Since the band gap of MnO (for bulk crystals E_g=4.2 eV) is higher than that of CuO (1.42 for the present work), the band gap of Mn-doped CuO should be greater than the band gap of pure CuO. The band gap values versus Mn-doping concentrations in the growth solution are plotted in Fig. 5.

4. Conclusions

Un-doped and Mn-doped CuO thin films were synthesized by the SILAR method. All of the films are crack free with nano-sized (plate-like) particles. From the SEM images it was also understood that the thickness and lengths of the plate-like nanostructures were affected by the Mn concentration. The EDS analysis showed that the Mn-doping percentages of the films had a linear dependence with the Mn^{+2} ion concentration in the growth solution. The XRD results showed that all of the films have polycrystalline nature with monoclinic structure. The UV–vis analysis suggested that the Mn-doping concentration in the films affected the transmission and optical band gap. As Mn concentration increases the optical transmission and optical band gap energy values also increase. Copper oxide and Mn are known to be perfect catalysts which implies that Mn doping to CuO can improve the catalytic properties of CuO.

References

[1] Iqbal Singh, R.K. Bedi, Studies and correlation among the structural, electrical and gas response properties of aerosol spray deposited self assembled nanocrystalline CuO, Applied Surface Science 257 (2011) 7592–7599.

[2] R. Sahay, J. Sundaramurthy, P. Suresh Kumar, V. Thavasi, S.G. Mhaisalkar, S. Ramakrishna, Synthesis and characterization of CuO nanofibers, and investigation for its suitability as blocking layer in ZnO NPs based dye sensitized solar cell and as photocatalyst in organic dye degradation, Journal of Solid State Chemistry 186 (2012) 261–267.

[3] Likun Zheng, Xinjian Liu, Solution-phase synthesis of CuO hierarchical nanosheets at near-neutral pH and near-room temperature, Materials Letters 61 (2007) 2222–2226.

[4] Rui Li, Jimin Du, Yuxia Luan, Yiguo Xue, Hua Zou, Guangshan Zhuang, Zhonghao Li, Ionic liquid precursor-based synthesis of CuO nanoplates for gas sensing and amperometric sensing applications, Sensors and Actuators B 168 (2012) 156–164.

[5] Kajal Jindal, Monika Tomar, Vinay Gupta, CuO thin film based uric acid biosensor with enhanced response characteristics, Biosensors and Bioelectronics 38 (2012) 11–18.

[6] Ho Chang, Mu-Jung Kao, Kun-Ching Cho, Sih-Li Chen, Kung-Hui Chu, Chieh-Chen Chen, Integration of CuO thin films and dye-sensitized solar cells for thermoelectric generators, Current Applied Physics 11 (2011) 19–22.

[7] T. Jarlborg, Effects of spin–phonon interaction within the CuO plane of high-T_c superconductors, Physica C 454 (2007) 5–14.

[8] Zhigang Yin, Yunhai Ding, Qingdong Zheng, Lunhui Guan, CuO/polypyrrole core–shell nanocomposites as anode materials for lithium-ion batteries, Electrochemistry Communications 20 (2012) 40–43.

[9] Suleman M. Inamdar, Vinod K. More, Sisir K. Mandal, CuO nanoparticles supported on silica, a new catalyst for facile synthesis of benzimidazoles, benzothiazoles and benzoxazoles, Tetrahedron Letters 54 (2013) 579–583.

[10] Sathish Reddy, B.E. Kumara Swamy, H. Jayadevappa, CuO nanoparticle sensor for the electrochemical determination of dopamine, Electrochimica Acta 61 (2012) 78–86.

[11] Zhibo Yang, Desheng Wang, Fei Li, Dequan Liu, Peng Wang, Xiuwan Li, Hongwei Yue, Shanglong Peng, Deyan He, Facile synthesis of CuO nanorod for lithium storage application, Materials Letters 90 (2013) 4–7.

[12] Wenli Gao, Shuhu Yang, Shaoguang Yang, Liya Lv, Youwei Du, Synthesis and magnetic properties of Mn doped CuO nanowires, Physics Letters A 375 (2010) 180–182.

[13] F. Bayansal, S. Kahraman, G. Çankaya, H.A. Çetinkara, H.S. Güder, H.M. Çakmak, Growth of homogenous CuO nanostructured thin films by a simple solution method, Journal of Alloys and Compounds 509 (2011) 2094–2098.

[14] Yuzeng Sun, Lin Ma, Baibin Zhou, Peng Gao, Cu(OH)$_2$ and CuO nanotube networks from hexaoxacyclooctadecane-like posnjakite microplates: synthesis and electrochemical hydrogen storage, International Journal of Hydrogen Energy 37 (2012) 2336–2343.

[15] Hongyan Cao, Xiaoshuang Li, Yaoqiang Chen, Maochu Gong, Jianli Wang, Effect of loading content of copper oxides on performance of Mn–Cu mixed oxide catalysts for catalytic combustion of benzene, Journal of Rare Earths 30 (2012) 871–877.

[16] S.G. Yang, T. Li, B.X. Gu, Y.W. Du, H.Y. Sung, S.T. Hung, C.Y. Wong, A.B. Pakhomov, Ferromagnetism in Mn-doped CuO, Applied Physics Letters 83 (2003) 3746–3748.

[17] Yaping Zhang, Liqing Pan, Yousong Gu, Fan Zhao, Hongmei Qiu, Jinhua Yin, Hao Zhu, John Q. Xiao, Metal–insulator transition in ferromagnetic Mn-doped CuO thin films, Journal of Applied Physics 105 (2009) 086103–086105.

[18] A. Ebrahimi, A. Pirouz, Y. Abdi, S. Azimi, S. Mohajerzadeh, Selective deposition of CuO/SnO$_2$ sol–gel on porous SiO$_2$ suitable for the fabrication of MEMS-based H$_2$S sensors, Sensors and Actuators B 173 (2012) 802–810.

[19] V.R. Katti, A.K. Debnath, K.P. Muthe, Manmeet Kaur, A.K. Dua, S.C. Gadkari, S.K. Gupta, V.C. Sahni, Mechanism of drifts in H$_2$S sensing properties of SnO$_2$:CuO composite thin film sensors prepared by thermal evaporation, Sensors and Actuators B 96 (2003) 245–252.

[20] Leilei Guo, Fang Tong, Haowen Liu, Hanmin Yang, Jinlin Li, Shape-controlled synthesis of self-assembly cubic CuO nanostructures by microwave, Materials Letters 71 (2012) 32–35.

[21] Liqiang Luo, Limei Zhu, Zhenxin Wang, Nonenzymatic amperometric determination of glucose by CuO nanocubes–graphene

nanocomposite modified electrode, Bioelectrochemistry 88 (2012) 156–163.
[22] F. Bayansal, H.A. Çetinkara, S. Kahraman, H.M. Çakmak, H.S. Güder, Nano-structured CuO films prepared by simple solution methods: plate-like, needle-like and network-like architectures, Ceramics International 38 (2012) 1859–1866.
[23] Durgajanani Sivalingam, Jeyaprakash Beri Gopalakrishnan, John Bosco, Balaguru Rayappan, Structural, morphological, electrical and vapour sensing properties of Mn doped nanostructured ZnO thin films, Sensors and Actuators B 166–167 (2012) 624–631.
[24] Xiaolu Yan, Dan Hu, Hangshi Li, Linxiao Li, Xiaoyu Chong, Yude Wang, Nanostructure and optical properties of M doped ZnO (M = Ni, Mn) thin films prepared by sol–gel process, Physica B 406 (2011) 3956–3962.